Fetal and Pediatric Pathology

ISSN: (Print) (Online) Journal homepage: www.tandfonline.com/journals/ipdp20

PAR2 Overexpression is Involved in the Occurrence of Hyperoxygen-Induced Bronchopulmonary Dysplasia in Rats

Chunyan Shao & Liqun Lu

To cite this article: Chunyan Shao & Liqun Lu (2023) PAR2 Overexpression is Involved in the Occurrence of Hyperoxygen-Induced Bronchopulmonary Dysplasia in Rats, Fetal and Pediatric Pathology, 42:3, 423-437, DOI: 10.1080/15513815.2023.2166799

To link to this article: https://doi.org/10.1080/15513815.2023.2166799

Published online: 19 Jan 2023.

FETAL AND PEDIATRIC PATHOLOGY
2023, VOL. 42, NO. 3, 423–437
https://doi.org/10.1080/15513815.2023.2166799

Taylor & Francis
Taylor & Francis Group

PAR2 Overexpression is Involved in the Occurrence of Hyperoxygen-Induced Bronchopulmonary Dysplasia in Rats

Chunyan Shao[a] and Liqun Lu[b]

[a]Department of Pediatrics, Chengdu Medical College, Chengdu, China; [b]Department of Pediatrics, The First Affiliated Hospital of Chengdu Medical College, Chengdu Medical College, Chengdu, China

ABSTRACT

Background: Bronchopulmonary dysplasia is a chronic lung disease commonly seen in preterm infants. It is characterized by delayed development of the alveoli and lung fibrosis. Protease-activated receptor 2 (PAR2) is an inflammatory driver that plays a proinflammatory role mainly through the P38 MAPK/NF-κB signaling pathway. **Methods:** Newborn rat pups were kept under air or oxygen at >60% concentration. Lung tissues were collected at postnatal days (P) 1, 4, 7, and 10 to observe pathological changes and take measurements. **Results:** In the hyperoxic group, P4 and P7 rats showed delayed alveolar development, septal thickening, and disturbances in alveolar structure.PAR2, P38 MAPK, NF-κB, and IL-18 expression at P4, P7, and P10 was significantly higher than in the air group. **Conclusion:** PAR2 is involved in lung injury induced by persistent hyperoxia. Activated PAR2 promotes IL-18 overexpression through the P38 MAPK/NF-κB signaling pathway, which may be an important mechanism of PAR2-mediated lung injury in bronchopulmonary dysplasia.

ARTICLE HISTORY
Received 5 September 2022
Revised 25 December 2022
Accepted 4 January 2023

KEYWORDS
Bronchopulmonary dysplasia; hyperoxia; protease-activated receptor 2 (PAR2); P38 MAPK; NF-κB

Introduction

Bronchopulmonary dysplasia (BPD) is a common chronic lung disease in premature infants with high mortality and complication rates that seriously affects the quality of life in later stages. The use of postnatal pulmonary surfactant and mechanically assisted ventilation improves the survival rate of premature infants, but long-term or inappropriate oxygen use can increase the frequency of BPD [1]. The pathogenesis of BPD remains unclear, but inflammation has been shown to be involved in its occurrence. Protease activated receptor-2 (PAR2) is a 7-time transmembrane G-protein coupled receptor, which is involved in the occurrence of a variety of lung diseases, such as lung inflammation and bronchial asthma, and is a driver of inflammatory response [2–4]. Activated PAR2 plays a pro-inflammatory role through a variety of signaling pathways. this study investigated the changes in the expression of PAR2, p38 mitogen-activated protein kinase (p38 MAPK), nuclear factor kappa B (NF-κB), and interleukin-18 (IL-18) in the lung tissues of hyperoxia-induced rat BPD models. The

CONTACT Liqun Lu luliqun7@sina.com Department of Pediatrics, The First Affiliated, Hospital of Chengdu Medical College, Chengdu Medical College, Chengdu, 610500, China

main aim of the study was to provide new insights into the pathogenesis of premature BPD to help develop preventative measures.

Materials and methods

Experimental animal grouping and model establishment

The use and care of experimental rodents was approved by the Animal Laboratory Center of the First Affiliated Hospital of Chengdu Medical College and the Animal Laboratory Management and Ethics Committee of the First Affiliated Hospital of Chengdu Medical College. All animal experiments complied with the ARRIVE guidelines and were carried out in accordance with the U.K. Animals (Scientific Procedures) Act, 1986 and associated guidelines, EU Directive 2010/63/EU for animal experiments, or the National Research Council's Guide for the Care and Use of Laboratory Animals.

Forty-eight pregnant Sprague–Dawley (SD) rats with a gestational age of 20–22 days were purchased from Chengdu Dasuo Company (Chengdu, China). The rats were randomly divided into a hyperoxia group and an air group, with 24 rats in each group. The neonatal SD rats in the hyperoxia group were kept in a closed oxygen chamber (provided by the laboratory of the First Affiliated Hospital of Chengdu Medical College) within 6 h after birth. A carbon dioxide and oxygen meter was used to monitor the oxygen concentration to ensure that it was continuously maintained at > 60% in the breeding cabin, to control the temperature in the cabin to 22–26 °C, and to maintain a humidity of 50–60%.

Newborn rats in both groups were fed by mothers who had recently delivered and were replaced with female rats in the air group every 24 h to avoid oxygen poisoning. Newborn rats in the air group were fed in the same room. The capsule was opened for 30 min every day, during which the bedding was replaced, food and drinking water were added, and the body weight, general condition, and deaths of SD rats in each group were recorded.

Specimen collection

From each group, six rats were randomly selected on day 1 (Postnatal 1, P1), day 4 (Postnatal 4, P4), day 7 (Postnatal 7, P7), and day 10 (Postnatal 10, P10). The rats were anesthetized by an intraperitoneal injection of 10% chloral hydrate. The rats were immediately sacrificed, and the chest cavity was opened. Lung tissues were removed to observe their appearance, and the lungs were rinsed three times with normal saline. After weighing, the right lung was frozen with liquid nitrogen and stored at −80 °C. The left lung was fixed with 4% paraformaldehyde for 24–48 h and then dehydrated and embedded.

Lung histopathological examination

The lung tissue was paraffin-embedded and sectioned at a thickness of 3–5 μm, following which hematoxylin-eosin (HE) and Masson staining were performed (all kits were purchased from Soleibo Biotechnology Co. Ltd., Beijing, China).

Radial alveolar counts (RAC)

Five sections were collected from each newborn SD rat and observed at 200× under a light microscope. A vertical line was made from the central part of the respiratory bronchiole to the nearest fibrous septum or pleura. The alveoli on this line were counted to determine the degree of alveolation, which can reflect the degree of lung development or injury. Each section was counted three times, and the average value was calculated.

Alveolar septal thickness

Six lung tissue sections were randomly selected from each group and observed at 400× under a light microscope. Three fields were randomly selected for each section, avoiding large vessels and the main bronchus. The alveolar septal thickness in each field was measured, and the average value was calculated.

Collagen fiber area of lung tissue

Masson staining was performed according to the Masson staining kit instructions, and then the staining area of collagen fibers in the lung tissue was measured. Eight lung tissue sections were randomly selected from each of the P4, P7, and P10 groups and observed at 400× under a light microscope. Three fields were randomly selected for each section, avoiding large vessels and the main bronchus. The ImageJ software was used to measure actual values and calculate the averages.

Expression of PAR2 and IL-18 using Western blotting

Frozen lung tissue was lysed, total protein was extracted with a protein extraction kit (Soleibo Biotechnology Company, Ltd, Beijing, China), and the protein concentration was determined. The proteins were separated by sodium dodecyl sulfate-polyacrylamide gel electrophoresis, semi-transferred to a polyvinylidene fluoride membrane, sealed for 2 h, and then mouse anti-PAR2 polyclonal antibody (dilution titer: 1:1000, SC-13504, SAM11, Santa Cruz Biotechnology, Dallas, TX, USA) and rabbit anti-IL-18 polyclonal antibody (dilution titer: 1:1500, DF6252, Affinity Biosciences, Ltd, Beijing, China) were added. These samples were then stored at 4 °C in a refrigerator overnight. After cleaning with Tris-HCl buffer salt solution, the bands were incubated with sheep anti-rat secondary antibodies (A0216, Abcam, Cambridge, UK) and sheep anti-rabbit secondary antibodies (S0001, Affinity Biosciences) at 22–24 °C for 2 h. Exposure to radiation and integral optical density (IOD) values were measured using ImageJ. Using β-actin as reference, the IOD ratio of the target band to the reference band was used as the relative protein expression.

Expression of PAR2, p38 MAPK, and NF-κB by immunohistochemistry

A Broad Spectrum Streptavidin-Peroxidase Immunohistochemical staining (SP) kit was purchased from Beijing Zhongshan Jinqiao Biotechnology Company, Ltd (Beijing, China). Paraffin tissue sections were routinely dehydrated, and following the

instructions of the SP kit, primary antibody against PAR2 (SC-13504, SAM11, Santa Cruz Biotechnology), p38 MAPK (BS-0637R, Bioss, Woburn, MA, USA), and NF-κB (AF506, Affinity Biosciences) were added, and the sections were incubated overnight in a refrigerator at 4 °C. The sections were rinsed with PBS and treated with the corresponding secondary antibody. Immunofluorescence was observed and photographed under a microscope. The positive staining area of PAR2, p38 MAPK, and NF-κB and total tissue area in the immunofluorescent images were analyzed and calculated by the ImageJ software. The corresponding positive staining area rate was obtained.

Statistical analysis

All experimental data are represented by the mean ± standard deviation ($\bar{X} \pm S$), and the SPSS26.0 software was used for statistical analysis. $P < 0.05$ indicated significance.

Results

Weight changes in rats from the two groups after birth

Compared with the air group, there was no significant difference in P1 body weight in the hyperoxia group ($p > 0.05$). With prolonged oxygen exposure, the rats gradually demonstrated slower weight gain, poor response, less activity, and weaker body shape. The body weights of rats in the P4, P7, and P10 hyperoxic groups were significantly lower than those in the air group ($p < 0.01$, $p < 0.01$, $p < 0.001$) (Table 1 and Figure 1).

Compared with that in the air group, the body weight growth rate of rats in the hyperoxic group decreased gradually with prolonged exposure to high oxygen ($p < 0.05$). ($^{*}p < 0.05$, $^{**}p < 0.01$, $^{***}p < 0.001$).

Table 1. Changes in the body weight (g) of the control and hyperoxia groups ($\bar{X} \pm S$).

Group	*P1*	*P4*	*P7*	*P10*
Control	7.54 ± 0.56	13.71 ± 1.08	19.52 ± 2.82	26.48 ± 2.02
Hyperoxia	7.35 ± 0.43	11.71 ± 0.73**	14.78 ± 0.70**	20.24 ± 1.03***

*$P < 0.05$, **$P < 0.01$, ***$P < 0.001$.

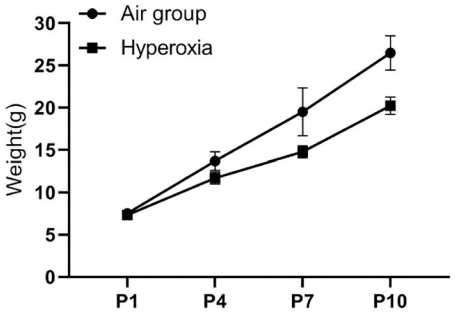

Figure 1. Comparison of the body weight between the air and hyperoxia groups at different time points.

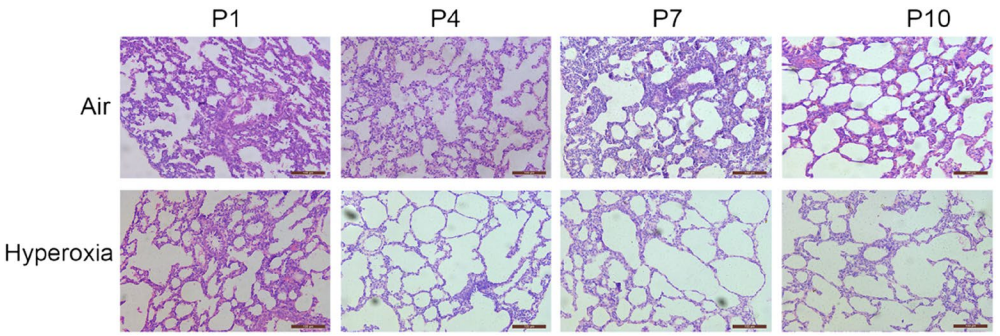

Figure 2. Lung tissue sections of rats in the air and hyperoxia groups at different time points (HE, 200×).

Table 2. Radial alveolar counts in the control and hyperoxia groups.

Group	*P1*	*P4*	*P7*	*P10*
Control	1.27 ± 0.80	4.67 ± 1.68	6.87 ± 1.30	9.80 ± 1.37
Hyperoxia	1.53 ± 0.83	2.33 ± 0.90***	4.53 ± 0.99***	5.27 ± 2.31***

*$P < 0.05$, **$P < 0.01$, ***$P < 0.001$.

Pathological changes in lung tissue in rats

HE staining of lung tissue

Observation under a light microscope showed that the P4 lung tissues of rats in the air group were still in the cystic stage—the number of terminal cavities gradually increased, and the alveolar septa became thicker. In the P7 air group, the number of alveoli increased slightly, and the alveolar septum became thinner. In the P10 group, the number of alveoli increased significantly, while the alveolar septum became significantly thinner. As the alveoli matured, their size remained uniform. The hyperoxia P4 group exhibited lung tissue edema, inflammatory cell infiltration, pulmonary septum rupture, and alveolar space expansion. The hyperoxia P7 group exhibited inflammatory cell infiltration, lung hemorrhage, and alveolar fusion. Lung tissue edema was more evident than in samples from previous timepoints, along with some lung space widening and lung tissue structure becoming disordered. This was more serious in the P7 group than in the P4 group. The hyperoxia P10 group exhibited lung tissue with evident alveolar structure disorder (Figure 2).

Compared with that of the air group, the alveoli of the hyperoxia P4 group were still in the vesicle stage. The development of alveoli was delayed due to alveolar dilation, inflammatory cell infiltration, and pulmonary septal rupture. In the P7 hyperoxia group, the alveolar cavity was further expanded, and alveolar fusion was observed. The lung tissue edema was more evident than before—part of the alveolar septum was widened, and lung tissue structure was disorganized. In the P10 hyperoxia group, the appearance of the pulmonary tissue deteriorated further, and the pulmonary alveolar structure disorder was evident.

Radial alveolar counts (RAC)

In the hyperoxia group, we observed that alveolar development stopped by day 7. Compared with the air group, the P1 group had no significant difference ($p > 0.05$),

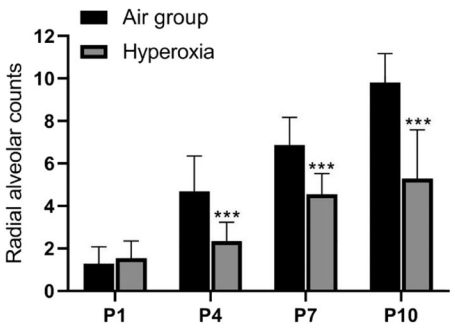

Figure 3. Radial alveolar count in the air and hyperoxia groups.

Table 3. Alveolar septal thickness in the control and hyperoxia groups (μm).

Group	*P1*	*P4*	*P7*	*P10*
Control	9.37 ± 1.84	10.47 ± 2.02	8.67 ± 2.16	9.62 ± 1.59
Hyperoxia	9.09 ± 2.45	11.10 ± 2.32	21.20 ± 5.83***	23.34 ± 5.97***

*$P < 0.05$, **$P < 0.01$, ***$P < 0.001$.

while P4, P7, and P10 groups had significant differences in RAC ($p < 0.001$ for all three groups) (Table 2 and Figure 3).

Compared with the air group, the radial alveolar count in the hyperoxia group was significantly lower in P4, P7, and P10 groups ($P < 0.001$). (*$p < 0.05$, **$p < 0.01$, ***$p < 0.001$).

Contrast of alveolar septal thickness

The results demonstrate that the thickness of the alveolar septa in the hyperoxia group increased gradually as the neonatal rats aged. In the P1 and P4 groups, there was no significant difference between the hyperoxia group and the air group. The alveolar septa in the hyperoxia P7 and P10 groups were significantly wider than those in the air group ($p < 0.001$) (Table 3 and Figure 4).

Compared to that in the air group, there was no significant difference in the thickness of alveolar septa in the hyperoxia group at P1 and P4 ($p > 0.05$). However, the thickness of alveolar septa increased significantly in the P7 and P10 groups ($p < 0.001$, $p < 0.001$). (*$p < 0.05$, **$p < 0.01$, ***$p < 0.001$).

Masson staining

Compared with that in the air group, the area of lung collagen fiber was significantly increased in the hyperoxia P7 and P10 groups ($p < 0.001$, $p < 0.001$). Pulmonary fibrosis was observed in the P7 and P10 group, while there was no significant difference in the P4 group ($p > 0.05$) (Figure 5a,b).

Compared to that in the air group, there was no significant difference in the collagen fiber staining area of the lung tissues in the hyperoxia P4 group ($p > 0.05$). However, the collagen fiber staining area was significantly increased in the P7 and P10 groups ($p > 0.001$, $p > 0.001$). (*$p < 0.05$, **$p < 0.01$, ***$p < 0.001$).

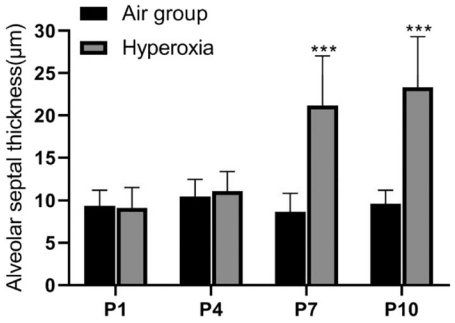

Figure 4. Alveolar septal thickness of rats in the air and hyperoxia groups.

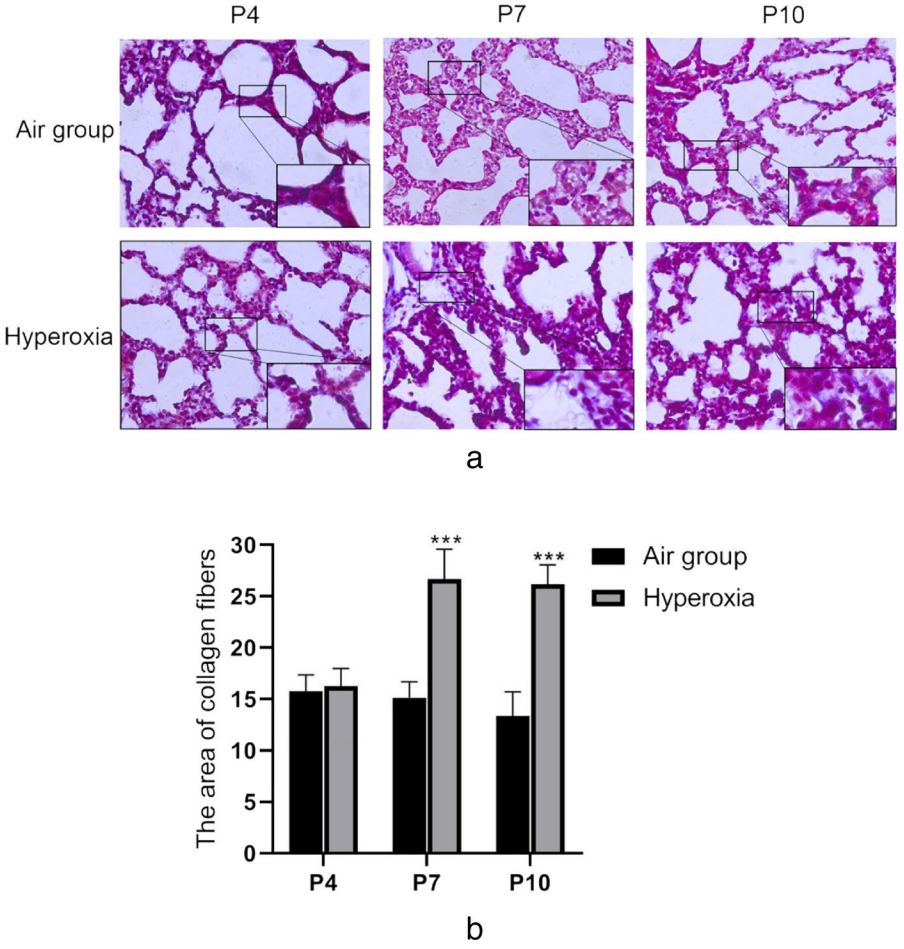

Figure 5. (a) Area of collagen fibers in lung tissues of rats in the air and hyperoxia groups (Masson, 400×). (b) Range of collagen fibre staining between the air and hyperoxia group.

Western blot analysis of PAR2 expression in lung tissue

Western blot analysis of PAR2 protein expression in rat lung tissues showed that there was no significant difference between the hyperoxia P1 group and the air group ($p > 0.05$), while P4, P7, and P10 groups showed increased expression ($p < 0.05$; $p < 0.01$; $p < 0.01$) (Figure 6a,b).

Compared with that in the air group, there was no significant difference in the expression of PAR2 in the lung tissues of the hyperoxia P1 group, but as the duration of oxygen exposure increased, the expression of PAR2 in the lung tissues of the hyperoxia groups (P4, P7, and P10) increased ($p > 0.05$, $p > 0.01$, $p > 0.01$). ($^{*}p < 0.05$, $^{**}p < 0.01$, $^{***}p < 0.001$).

Immunohistochemistry was used to detect the expression of PAR2 in lung tissues harvested on different days

The results of immunohistochemistry of lung tissues for PAR2 showed that compared to that in the air group, the PAR2 expression in the hyperoxia P1 group had no significant difference ($p > 0.05$), while the P4, P7, and P10 hyperoxia groups showed significantly increased PAR2 expression ($p < 0.001$) (Figure 6c,d).

Compared to that in the air group, there was no difference in the expression of PAR2 in the hyperoxia P1 group. The area of PAR2 expression in the hyperoxia P4, P7, and P10 groups was significantly increased ($p > 0.001$, $p > 0.001$, $p > 0.001$). ($^{*}p < 0.05$, $^{**}p < 0.01$, $^{***}p < 0.001$).

p38 MAPK expression was measured in lung tissues

Compared to that in the air group, there was no difference in the expression of p38 MAPK in hyperoxia P1 lung tissues ($p < 0.05$). However, the expression of p38 MAPK in hyperoxia P4, P7, and P10 lung tissues was significantly increased ($p < 0.001$) (Figure 7a,b).

Compared to that in the air group, there was no difference in the expression of p38 MAPK in the hyperoxia P1 group. However, the positive expression area in the hyperoxia P4, P7, and P10 groups was significantly increased ($p > 0.001$, $p > 0.001$, $p > 0.001$). ($^{*}p < 0.05$, $^{**}p < 0.01$, $^{***}p < 0.001$).

Expression of NF-κB in lung tissues

Compared to that in the air group, there was no difference in the expression of NF-κB in the lung tissues in the hyperoxia P1 group ($p > 0.05$), while the expression of NF-κB in the lung tissues of the hyperoxia P4, P7, and P10 groups was significantly increased ($p < 0.001$) (Figure 8a,b).

Compared with that in the air group, there was no difference in NF-κB expression in the hyperoxia P1 group, and the positive expression area of hyperoxia P4, P7, and P10 groups was significantly increased ($p > 0.001$, $p > 0.001$, $p > 0.001$). ($^{*}p < 0.05$, $^{**}p < 0.01$, $^{***}p < 0.001$).

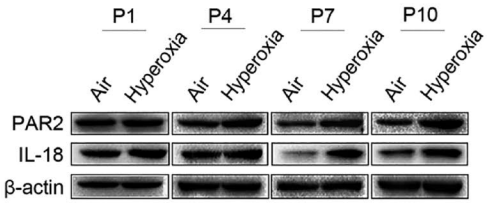

a

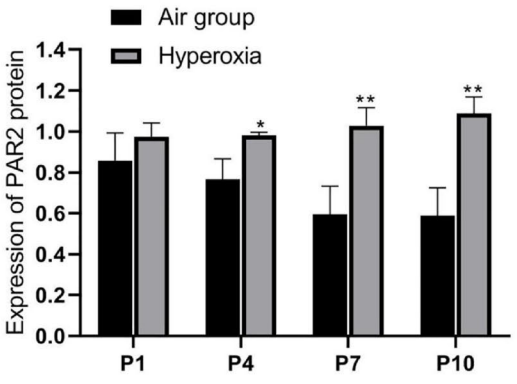

b

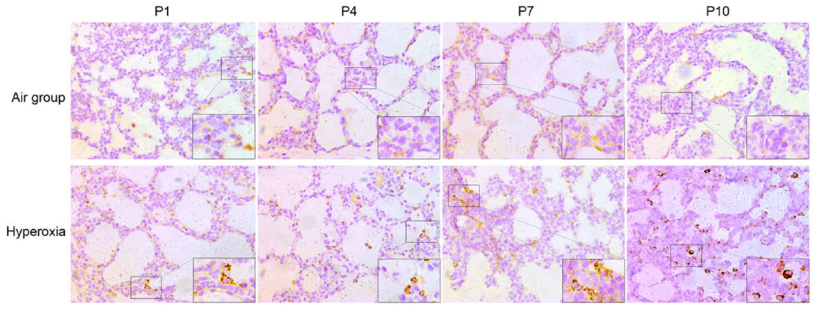

c

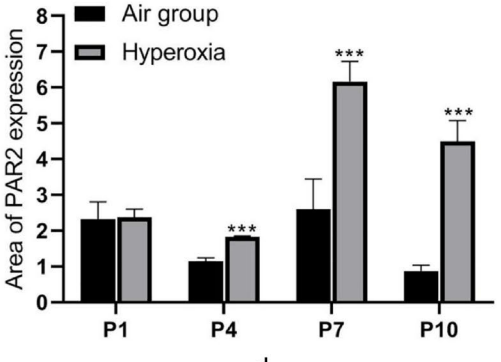

d

Figure 6. (a) PAR2 and IL-18 protein expression in lung tissues of rats in the air and hyperoxia groups. (b) PAR2 protein expression in lung tissues of rats in the air and hyperoxia groups. (c) Expression of PAR2 in lung tissues of rats in the air and hyperoxia groups (IHC, 400×). (d) Comparison of PAR2 expression area in lung tissues of the air and hyperoxia groups.

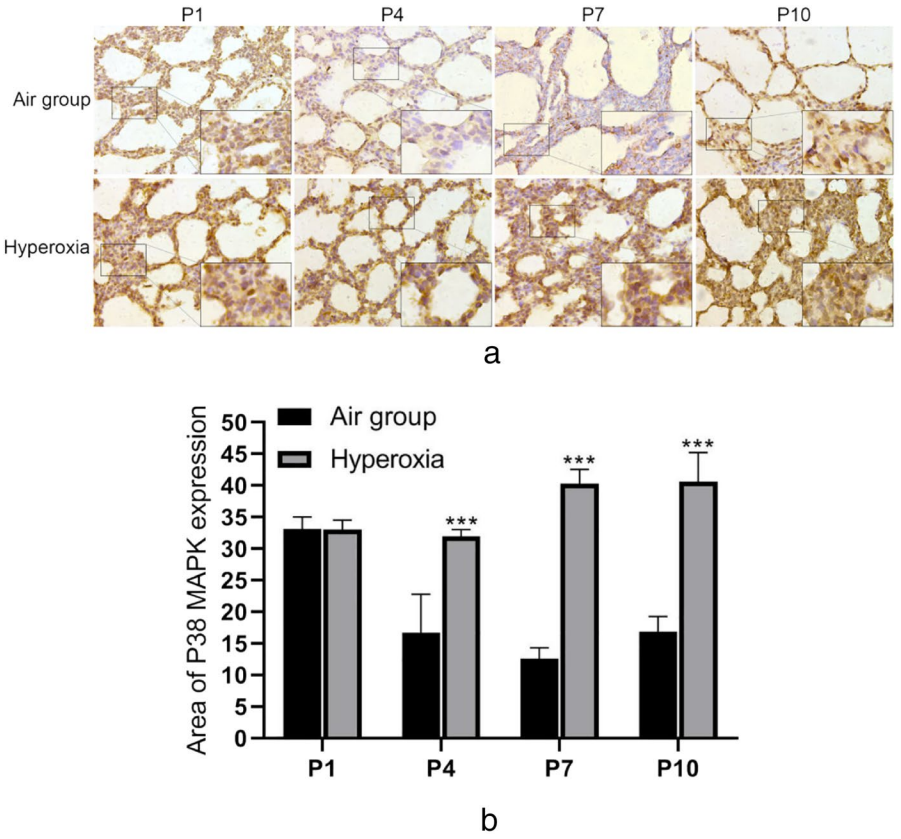

Figure 7. (a) Expression of p38 MAPK in lung tissues of rats in the air and hyperoxia groups (IHC, 400×). (b) Comparison of expression area of p38 MAPK in lung tissues between the air and hyperoxia groups.

Expression of IL-18 in lung tissues

Compared to that in the air group, there was no difference in the expression of IL-18 in lung tissues in the hyperoxia P1 group ($p > 0.05$), while the expression of IL-18 in lung tissue of the hyperoxia P4, P7, and P10 groups was increased ($p < 0.05$) (Figures 6a and 9).

Compared to that in the air group, there was no difference in the expression of IL-18 protein in the hyperoxia P1 group, while the expression in the hyperoxia P4, P7, and P10 groups was increased ($p > 0.05$, $p > 0.05$, $p > 0.05$). ($^{*}p < 0.05$, $^{**}p < 0.01$, $^{***}p < 0.001$).

Discussion

Lung development in rats is similar to that in humans. Specifically, the lung development in 3-day-old rats is comparable to that in premature infants at about 28 weeks [5–7]. The lung histopathology in rats exposed to a hyperoxygenated environment is similar to that of the lungs of infants with premature BPD [8]. This study used increased oxygen exposure to generate a newborn rat BPD model. The pathogenesis of BPD is highly complex, with inflammation playing a major role. A variety of

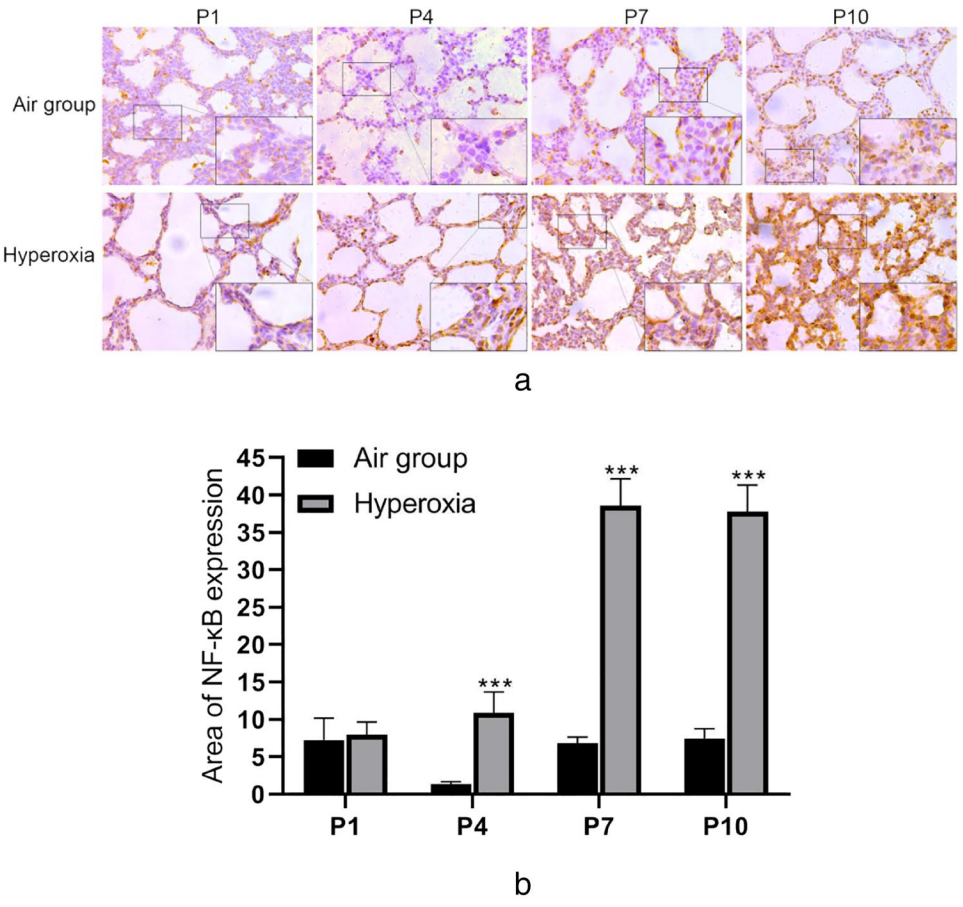

Figure 8. (a) Expression of NF-κB in lung tissues of rats in the air and hyperoxia groups (IHC, 400×). (b) Comparison of NF-κB expression area in lung tissues between the air and hyperoxia groups.

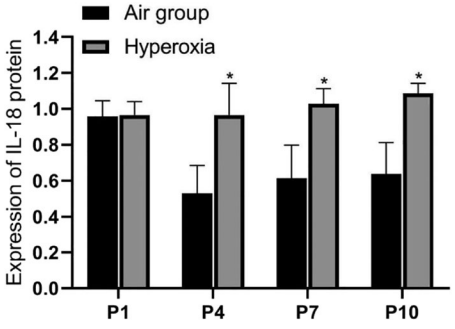

Figure 9. IL-18 protein expression in lung tissues of rats in the air and hyperoxia groups.

post-birth environmental factors, such as infection and oxygen therapy, can trigger a continuous pro-inflammatory disorder of the lung immune system in premature deliveries, which leads to the stagnation of lung development and the reduction in alveolarization and vascularization [9]. In the present study, we observed that with prolonged

oxygen exposure time, the growth and development of rats were retarded, inflammatory cell infiltration, alveolar development arrest, and alveolar septal thickening occurred in the lungs, and collagen fiber hyperplasia occurred after P7, indicating the formation of pulmonary fibrosis, which is similar to the pathological manifestations of premature BPD.

PAR2, a member of the g-protein-coupled receptor family, can be irreversibly activated by a variety of proteolytic enzymes, among which trypsin is the most active [3,10]. PAR2 is widely expressed in a variety of lung and respiratory cells, including vascular smooth muscle cells, airway endothelial and epithelial cells, fibroblasts, mast cells, eosinophils, and alveolar macrophages [11]. PAR2 mediates inflammatory reactions and is involved in the occurrence of a variety of lung diseases, such as pneumonia, cystic fibrosis, acute lung injury, adult respiratory distress syndrome, and chronic obstructive pulmonary disease [12–14]. Small et al. [13] found that the inhibition of PAR2, the target protein of cathepsin S, leads to reduced airway inflammation and mucin expression in transgenic mice overexpressing β-epithelial Na^+ channels (a cystic fibrosis pulmonary disease model), suggesting that the receptor plays a role in cathepsin-induced pulmonary fibrosis. Previous research has demonstrated that PAR2 is overexpressed in the lung tissues of patients with idiopathic pulmonary fibrosis and can mediate the proliferation of human lung fibroblasts in vitro [15]. The expression of PAR2 and transforming growth factor-β increases in bleomycin-induced pulmonary fibrosis in rats, further confirming the role of PAR2 in experimental fibrosis [16]. In human bronchial epithelial cells, cigarette extract enhances the production of inflammatory factors induced by neutrophil elastase through the upregulation of PAR2 [17]. We hypothesized that PAR2 may be involved in lung injury and lung fiber formation in BPD. To clarify the relationship between PAR2 and BPD, we measured the expression of PAR2 in the lung tissues of BPD rats on different postnatal days and found that PAR2 was highly expressed in the hyperoxia P4, P7, and P10 groups, suggesting that PAR2 is involved in the occurrence of hyperoxia-induced BPD.

IL-18 is considered to be an effective pro-inflammatory cytokine, which exists in activated macrophages and epithelial cells and can regulate autoimmune and inflammatory diseases [18,19]. Ikawa et al. [20] found that neutrophil recruitment and neutrophil serine protease activation of PAR2 play important roles in the induction of IL-18, as well as IL-18-dependent liver injury in vivo. It has also been found that urinary tract infections can lead to the release of IL-18 exosomes and promote the migration of mast cells. The trypsin secreted by mast cells acts on PAR2, aggravating damage to the urinary epithelial barrier function [21]. Caffeine has a strong anti-inflammatory effect and is a common drug in the clinical treatment of BPD. This drug was found to reduce the secretion of IL-1β and IL-18 in human monocytic leukemia cell line (THP-1) macrophages and significantly reduce the phosphorylation levels of MAPK and NF-κB pathway members, inhibiting the translocation of NF-κB in THP-1 macrophages [22]. Previous studies have shown that lipopolysaccharide stimulation of MAPK and NF-κB pathways is the first sign of IL-18 transcription up-regulation in macrophages [22,23].

We have confirmed the relationship between PAR2 and BPD. To further explore whether PAR2 can act on BPD lung injury through a pro-inflammatory reaction, we measured the expression of IL-18 in lung tissues and found that IL-18 release increased

in the hyperoxia P4, P7, and P10 groups, and showed a synergistic relationship with PAR2. Hyperoxia can stimulate the expression of PAR2 and IL-18. Combining our results with those of previous studies, we hypothesized that activated PAR2 mediates the p38 MAPK/NF-κB signaling pathway in hyperoxia-induced BPD lung injury, thereby promoting the up-regulation and release of IL-18 in macrophages, which induces the activation of PAR2.

Activated PAR2 induces classical signal transduction pathways by directly coupling with G-protein, leading to the rapid transcription of inflammation-related genes [24]. To further elucidate the specific signaling pathway of PAR2 in BPD lung injury, we detected the expression of p38 MAPK and NF-κB in the hyperoxia group at different postnatal days, and found that the expression in the P4, P7, and P10 groups was increased, indicating that PAR2 acts through the p38 MAPK/NF-κB signaling pathway in the BPD model. PAR2, a driver of inflammatory response, is associated with proliferative cell responses through the p38 MAPK-mediated signaling pathway and with inflammation through the NF-κB pathway [3,24]. Trypsin-activated PAR2 mediates the expression and secretion of many inflammatory mediators by activating NF-κB [25]. PAR2 antagonists can reduce the expression of p-p38, p-IκBα, and p-NF-κB in vitro. Down-regulated PAR2 can also improve osteoarthritis in rats by regulating the MAPK/NF-κB signaling pathway [26]. NF-κB activation has also been demonstrated through a synergistic effect of PAR2 and toll-like receptor 4 (TLR4), whose ectopic co-expression leads to an increase in the activity of the NF-κB signaling pathway induced by PAR2 agonists, resulting in proinflammatory cytokine production [27]. PAR2 regulates cytokine release in gastrointestinal cells through ERK/RSK p90, NF-κB phosphorylation, and histone acetyltransferase activity, and stimulates up-regulation of inflammatory factor transcription in colon epithelial cells [28]. Recent research has also found that insulin, as an anti-inflammatory agent, can regulate PAR2-induced acute inflammatory response by reducing leukocyte recruitment and inflammation in mouse paw edema models [29].

In conclusion, this study preliminarily demonstrated that PAR2 overexpression may be related to the formation of pulmonary fibrosis in rats with hyperoxia-induced BPD, which can induce lung injury in BPD by enhancing the expression of the inflammatory factor IL-18; the P38 MAPK/NF-κB signaling pathway may be involved in this mechanism. In the future, a series of experiments will be conducted using knockout animals to further elucidate the relationship between PAR2 and BPD and the specific pathogenesis. This study provides new ideas on the exploration of BPD pathogenesis. However, the relationship between PAR2 and hyperoxic lung injury requires further study.

Acknowledgments

We would like to thank the Experimental Center of the First Affiliated Hospital of Chengdu Medical College.

Disclosure statement

No potential conflict of interest was reported by the author(s).

Funding

This research was supported by the Sichuan Province Medical Research Project (grant number S21007), the Sichuan Province Applied Basic Research Project (grant number 2022NSFSC0787), and the Chengdu Medical Research Project (grant number 2021216).

Data availability statement

Data supporting the results or analyzed in this paper are available at https://data.mendeley.com/drafts/dkj3xnffp7

References

[1] Mohammadizadeh M, Ardestani AG, Sadeghnia AR. Early administration of surfactant via a thin intratracheal catheter in preterm infants with respiratory distress syndrome: feasibility and outcome. J Res Pharm Pract. 2015;4:31–6. doi:10.4103/2279-042X.150053.

[2] Chandrabalan A, Ramachandran R. Molecular mechanisms regulating proteinase-activated receptors (PARs). FEBS J. 2021;288(8):2697–726. Cited in: PMID: 33742547. doi:10.1111/febs.15829.

[3] de Almeida AD, Silva IS, Fernandes-Braga W, LimaFilho ACM, Florentino ROM, Barra A, de Oliveira Andrade L, Leite MF, Cassali GD, Klein A. A role for mast cells and mast cell tryptase in driving neutrophil recruitment in LPS-induced lung inflammation via protease-activated receptor 2 in mice. Inflamm Res. 2020;69(10):1059–70. doi:10.1007/s00011-020-01376-4.

[4] Asaduzzaman M, Davidson C, Nahirney D, Fiteih Y, Puttagunta L, Vliagoftis H. Proteinase-activated receptor-2 blockade inhibits changes seen in a chronic murine asthma model. Allergy. 2018;73(2):416–20. doi:10.1111/all.13313.

[5] Pinkerton KE, Joad JP. The mammalian respiratory system and critical windows of exposure for children's health. Environ Health Perspect. 2000;108 (Suppl 3):457–62. doi:10.1289/ehp.00108s3457.

[6] Burri PH. Structural aspects of postnatal lung development – alveolar formation and growth. Biol Neonate. 2006;89(4):313–22. Cited in: PMID: 16770071. doi:10.1159/000092868.

[7] Chu X, Zhang X, Gong X, Zhou H, Cai C. Effects of hyperoxia exposure on the expression of Nrf2 and heme oxygenase-1 in lung tissues of premature rats. Mol Cell Probes. 2020;51:101529. doi:10.1016/j.mcp.2020.101529.

[8] Jobe AH. What is BPD in 2012 and what will BPD become? Early Hum Dev. 2012;88:S27–S28. doi:10.1016/S0378-3782(12)70009-9.

[9] Thébaud B, Goss KN, Laughon M, Whitsett JA, Abman SH, Steinhorn RH, Aschner JL, Davis PG, McGrath-Morrow SA, Soll RF, et al. Bronchopulmonary dysplasia. Nat Rev Dis Primers. 2019;5:78. doi:10.1038/s41572-019-0127-7.

[10] Macfarlane SR, Seatter MJ, Kanke T, Hunter GD, Plevin R. Proteinase-activated receptors. Pharmacol Rev. 2001;53(2):245–282.

[11] Schmidt VA, Nierman WC, Feldblyum TV, Maglott DR, Bahou WF. The human thrombin receptor and proteinase activated receptor-2 genes are tightly linked on chromosome 5q13. Br J Haematol. 1997;97(3):523–9. doi:10.1046/j.1365-2141.1997.922907.x.

[12] Moraes TJ, Martin R, Plumb JD, Vachon E, Cameron CM, Danesh A, Kelvin DJ, Ruf W, Downey GP. Role of PAR2 in murine pulmonary pseudomonal infection. Am J Physiol Lung Cell Mol Physiol. 2008;294(2):L368–L377. doi:10.1152/ajplung.00036.2007.

[13] Small DM, Brown RR, Doherty DF, Abladey A, Zhou-Suckow Z, Delaney RJ, Kerrigan L, Dougan CM, Borensztajn KS, Holsinger L, et al. Targeting of cathepsin S reduces cystic fibrosis-like lung disease. Eur Respir J. 2019;53:1801523. doi:10.1183/13993003.01523-2018. Cited in: PMID: 30655278.

[14] Ramachandran R, Morice AH, Compton SJ. Proteinase-activated receptor2 agonists upregulate granulocyte colony-stimulating factor, IL-8, and VCAM-1 expression in human bronchial fibroblasts. Am J Respir Cell Mol Biol. 2006;35(1):133–41. doi:10.1165/rcmb.2005-0362OC.
[15] Wygrecka M, Kwapiszewska G, Jablonska E, von Gerlach S, Henneke I, Zakrzewicz D, Guenther A, Preissner KT, Markart P. Role of protease-activated receptor-2 in idiopathic pulmonary fibrosis. Am J Respir Crit Care Med. 2011;183(12):1703–14. doi:10.1164/rccm.201009-1479OC.
[16] Syamala S, Thomas D, Srinivasan K, Narayanan S, Ganapasam S. Daidzein exhibits anti-fibrotic effect by reducing the expressions of proteinase activated receptor 2 and TGFβ1/smad mediated inflammation and apoptosis in Bleomycin-induced experimental pulmonary fibrosis. Biochimie. 2014;103:23–36. doi:10.1016/j.biochi.2014.04.005.
[17] Lee KH, Lee J, Jeong J, Woo J, Lee CH, Yoo CG. Cigarette smoke extract enhances neutrophil elastase-induced IL-8 production via proteinase-activated receptor-2 upregulation in human bronchial epithelial cells. Exp Mol Med. 2018;50(7):1–9. doi:10.1038/s12276-018-0114-1.
[18] Dinarello CA, Fantuzzi G. Interleukin-18 and host defense against infection. J Infect Dis. 2003;187 Suppl 2:S370–S384. doi:10.1086/374751.
[19] Gracie JA, Robertson SE, McInnes IB. Interleukin-18. J Leukoc Biol. 2003;73(2):213–24. Cited in: PMID: 12554798. doi:10.1189/jlb.0602313.
[20] Ikawa K, Nishioka T, Yu Z, Sugawara Y, Kawagoe J, Takizawa T, Primo V, Nikolic B, Kuroishi T, Sasano T, et al. Involvement of neutrophil recruitment and protease-activated receptor 2 activation in the induction of IL-18 in mice. J Leukoc Biol. 2005;78(5):1118–26. doi:10.1189/jlb.0305151.
[21] Wu Z, Li Y, Liu Q, Liu Y, Chen L, Zhao H, Guo H, Zhu K, Zhou N, Chai TC, et al. Pyroptosis engagement and bladder urothelial cell-derived exosomes recruit mast cells and induce barrier dysfunction of bladder urothelium after uropathogenic *E. coli* infection. Am J Physiol Cell Physiol. 2019;317(3):C544–C555. doi:10.1152/ajpcell.00102.2019.
[22] Zhao W, Ma L, Cai C, Gong X. Caffeine inhibits NLRP3 inflammasome activation by suppressing MAPK/NF-κB and A2aR signaling in LPS-induced THP-1 macrophages. Int J Biol Sci. 2019;15(8):1571–81. doi:10.7150/ijbs.34211.
[23] Oeckinghaus A, Hayden MS, Ghosh S. Crosstalk in NF-κB signaling pathways. Nat Immunol. 2011;12(8):695–708. Cited in: PMID: 21772278. doi:10.1038/ni.2065.
[24] Steinhoff M, Buddenkotte J, Shpacovitch V, Rattenholl A, Moormann C, Vergnolle N, Luger TA, Hollenberg MD. Proteinase-activated receptors: transducers of proteinase-mediated signaling in inflammation and immune response. Endocr Rev. 2005;26(1):1–43. doi:10.1210/er.2003-0025.
[25] Rudack C, Steinhoff M, Mooren F, Buddenkotte J, Becker K, von Eiff C, Sachse F. PAR-2 activation regulates IL-8 and GRO-alpha synthesis by NF-kappaB, but not RANTES, IL-6, eotaxin or TARC expression in nasal epithelium. Clin Exp Allergy. 2007;37(7):1009–22. doi:10.1111/j.1365-2222.2007.02686.x.
[26] Yan S, Ding H, Peng J, Wang X, Pang C, Wei J, Wei J, Chen H. Down-regulation of protease-activated receptor 2 ameliorated osteoarthritis in rats through regulation of MAPK/NF-κB signaling pathway in vivo and in vitro. Biosci Rep. 2020;40:BSR20192620. doi:10.1042/BSR20192620.
[27] Nhu QM, Shirey K, Teijaro JR, Farber DL, Netzel-Arnett S, Antalis TM, Fasano A, Vogel SN. Novel signaling interactions between proteinase-activated receptor 2 and toll-like receptors in vitro and in vivo. Mucosal Immunol. 2010;3(1):29–39. doi:10.1038/mi.2009.120.
[28] Wang H, Moreau F, Hirota CL, MacNaughton WK. Proteinase-activated receptors induce interleukin-8 expression by intestinal epithelial cells through ERK/RSK90 activation and histone acetylation. FASEB J. 2010;24(6):1971–80. doi:10.1096/fj.09-137646.
[29] Hyun E, Ramachandran R, Cenac N, Houle S, Rousset P, Saxena A, Liblau RS, Hollenberg MD, Vergnolle N. Insulin modulates protease-activated receptor 2 signaling: implications for the innate immune response. J Immunol. 2010;184(5):2702–9. doi:10.4049/jimmunol.0902171.